Supplementary Information

Bio-inspired Design of Hierarchical PDMS Microstructures with Tunable Adhesive Superhydrophobicity

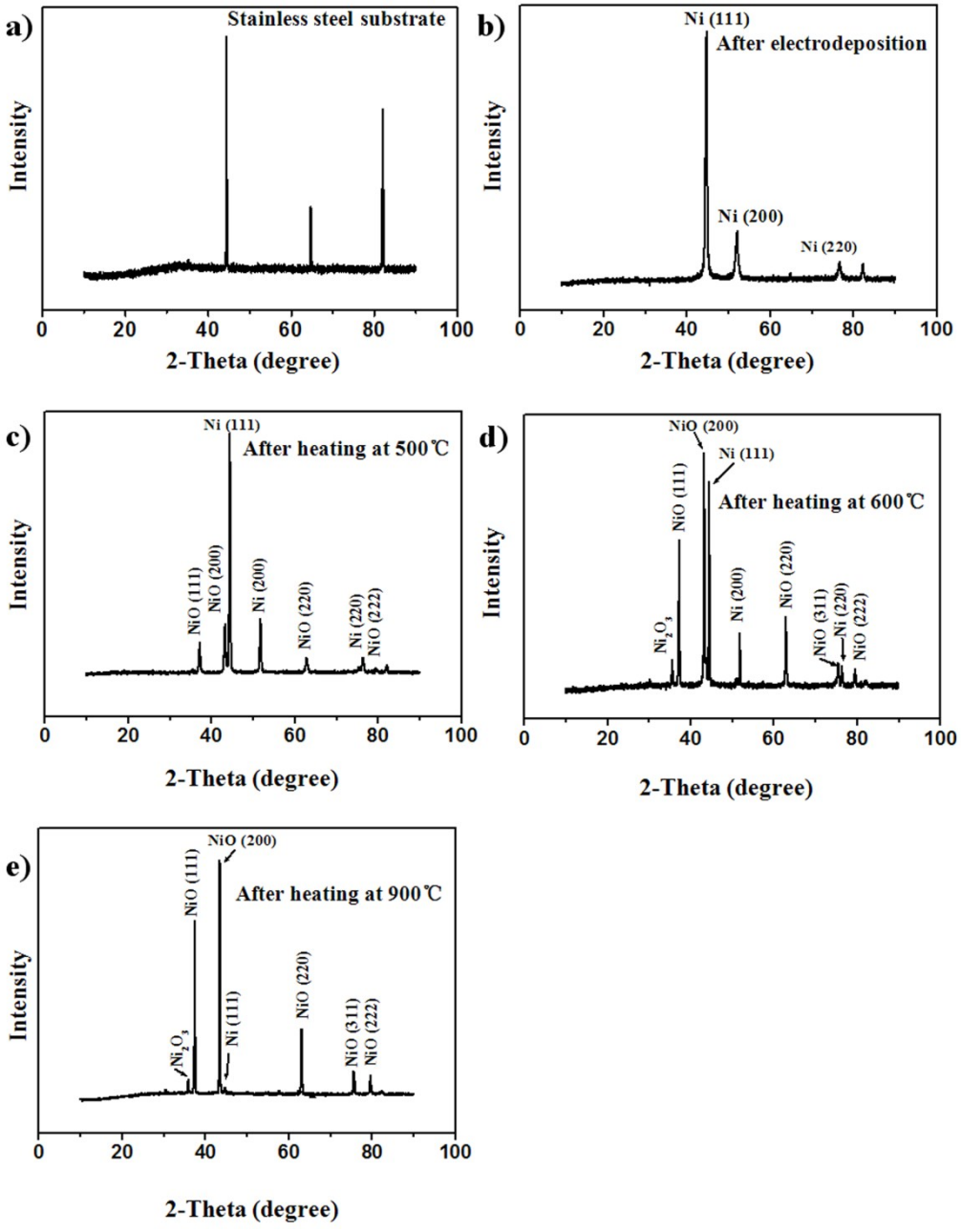

Figure S1. XRD result of stainless steel sheet, Ni and porous Ni/NiO templates annealed at different temperatures.

X-ray diffraction (XRD) was carried out using a D8 Advance (Bruker) with Cu Ka radiation (λ=0.15405 nm). Before electro-deposition, only peaks ascribed to stainless steel can be observed. After electro-deposition, the peaks attributed to Ni arise. After

heating at different temperatures, some new peaks ascribed to NiO appear. The Ni/NiO templates after annealing have been successfully prepared and no peaks relating to other phases are observed.

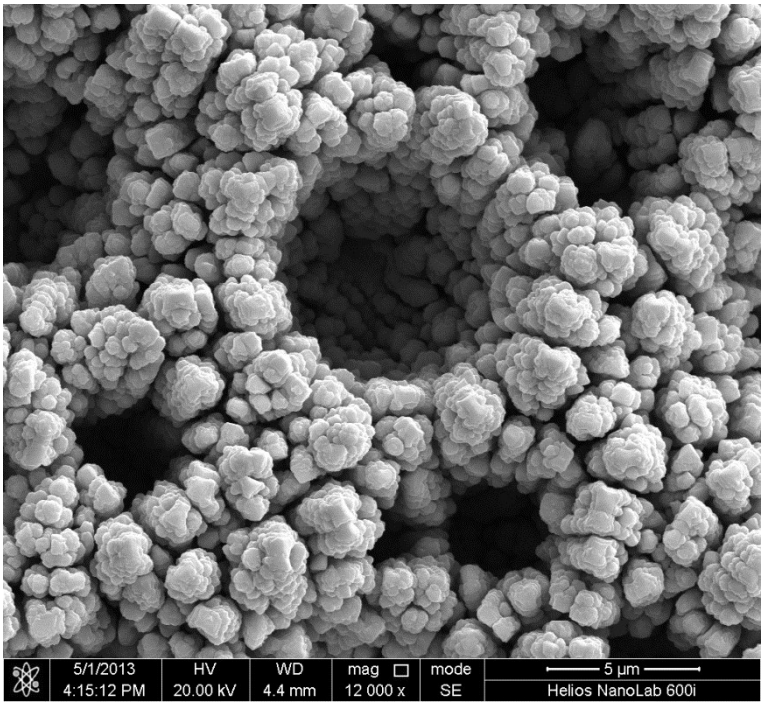

Figure S2. SEM image of the porous Ni obtained after electro-deposition without annealing.

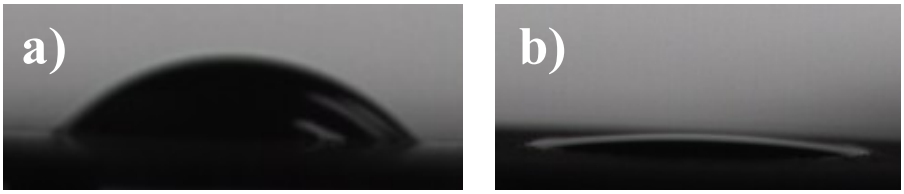

Figure S3. Shapes of a PDMS prepolymer on the hierarchical (a) Ni surface and (b) Ni/NiO surface (obtained after heating at 500 °C). The PDMS prepolymer has a lower contact angle on the Ni/NiO surface, which can facilitate the entering of the prepolymer into the templates.

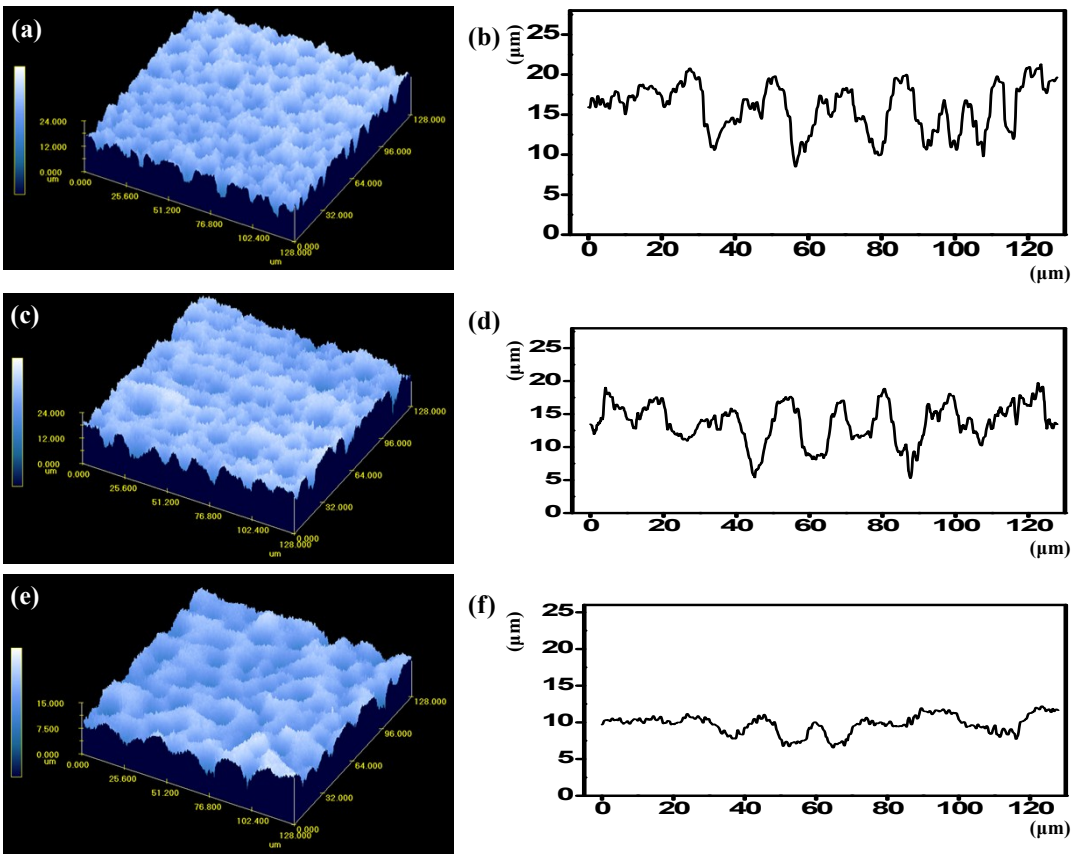

Figure S4. Confocal microscopy images: 3D images for Ni/NiO microstructures obtained at (a) 500 °C, (c) 600 °C, and (e) 900 °C, respectively. (b), (d), and (f) are the profiles pictures for (a), (c), and (e), respectively.

Based on the confocal microscopy images, it can be noticed that the depth of pore decreases with the increase of heating temperature. The corresponding profile pictures show that the average depth decreases from about 8.6 µm to 4.7 µm. The variation of surface morphology and microstructure scale is attributed to the oxidation of Ni to NiO during the heating process. [1]

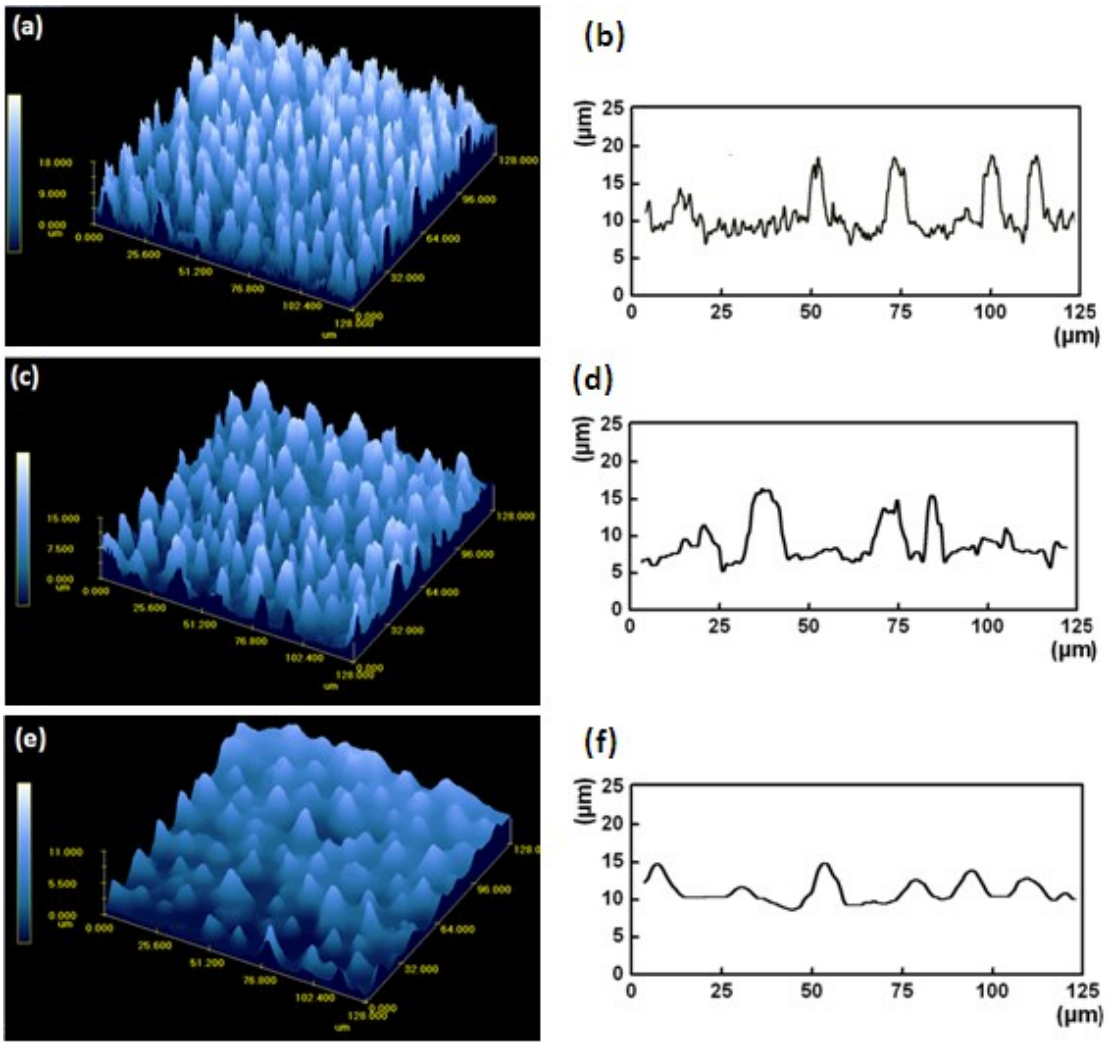

Figure S5. Confocal microscopy images: 3D images for PDMS samples (a) S1, (c) S2 and (e) S3, respectively; (b), (d), and (f) are the profiles pictures for (a), (c), and (e), respectively. It can be noticed that the microstructures for different samples vary and this is consistent with the SEM results.

Discussion of the super-hydrophobicity on the as-prepared PDMS films:

A flat PDMS film was prepared as the control sample and its water contact angle is only about 105° (Figure 4). In this work, all of the as-prepared films have the super-hydrophobicity (the contact angles higher than 150°), and such high hydrophobicity can be ascribed to the enhanced effect of the hierarchical micro/nanostructures on the hydrophobicity. On the as-prepared films, although water droplets reside in different states (Figure 6, S1: lotus state; S2: Cassie stat; S3: Cassie impregnating wetting state), the interface under water involves both solid PDMS and air layer (Figure 6). Therefore, the high hydrophobicity can be explained by the as the following equation, which was proposed by Cassie and Baxter:[2]

$$\cos\theta_r = f_1 \cos\theta - f_2 \qquad (1)$$

Herein, (θ) and (θ_r) are the contact angles of the flat PDMS and the rough PDMS films, respectively, f_1 and f_2 are the fractions of the solid surface and air layer in contact with water, respectively (i.e., $f_1 + f_2 = 1$). Deduced from the above equation, increasing f_2 will lead to the increase of θ_r, which means the fraction of air trapped under water is an important factor in determining the super-hydrophobicity of the surface. In this work, θ = 105° (see Figure 4), for sample S1, S2 and S3, and θ_r are 158°, 154°, and 151°, respectively. According to equation 1, f_2 can be calculated to be 0.902, 0.863, and 0.831, respectively, indicating that the fraction of air is high enough to result in super-hydrophobicity. Furthermore, the f_2 decreases when the wetting states change from lotus state for sample S1 to the Cassie impregnating wetting state for sample S3, indicating that the solid-liquid contact fraction f_1 increases. Therefore, the adhesion increases and the wetting states change because of the variation of solid-liquid contact area.

References

1. L. D. L. S. Valladares, A. Ionescu, S. Holmes, C. H. W. Barnes, A. B. Domínguez, O. A. Quispe, J. C. González, S. Milana, M. Barbone, A. C. Ferrari, H. Ramos, Y. Majima, *J. Vac. Sci. Technol. B* 2014, **32**, 051808.
2. A. B. D. Cassie and S. Baxter, *Trans. Faraday Soc*, 1944, **40**, 546.